Optimization of Linear Flux Switching Permanent Magnet Motor

W. Min[1,2], J. T. Chen[2], Z. Q. Zhu[2], Y.Zhu[1],G. H. Duan[1]
[1]Institute of Manufacturing Engineering, Department of Precision Instruments and Mechanology, Tsinghua University, Beijing, 100084, China.
[2]Department of Electronic & Electrical Engineering, University of Sheffield, Sheffield S1 3JD, U.K.
zzp09wm@sheffield.ac.uk, J.Chen@sheffield.ac.uk, Z.Q.Zhu@sheffield.ac.uk,
zhuyu@tsinghua.edu.cn, duangh@tsinghua.edu.cn

***Abstract*-Linear planar flux-switching permanent magnet (FSPM) brushless machines have significant potential for transportation application. A 6-slot/5-pole linear FSPM motor is optimized in this paper for maximum thrust force at a fixed copper loss and also for minimum cogging force by finite element (FE) analysis. The influence of major design parameters, such as the split ratio between the mover and stator, the stator pole width, the stator pole height, the mover back-iron thickness and the mover tooth width, on the thrust force, when the copper loss is fixed, is firstly investigated by individual parameter optimization. The results are then compared to a global optimization of thrust force obtained by genetic algorithm. It is shown that their differences are very small and hence the individual parameter optimization may be employed in optimizing such linear FSPM motor. Finally, the peak-to-peak value of the cogging force is reduced by ~40% via optimizing the slot opening and width associated with the end teeth.**

I. INTRODUCTION

Linear flux-switching permanent magnet (FSPM) machines inherit all the merits of the rotary FSPM machines, such as unique armature structure, simple and robust mover or stator structure, and are suitable for high force and high electric loading applications where linear movements are needed, e.g. transportation, automobile and aerospace. Particularly, linear FSPM machines are attractive for long-stroke applications, since, as in Sawyer motors [1] and [2], both magnets and coils can be mounted on the short mover so that less permanent magnets or copper will be used than the conventional long-stroke linear PM machines, which will significantly reduce the cost. Therefore, linear FSPM machines have received increasing attention in the academic and industrial field [3]-[6].

In order to obtain high force density and efficiency, individual parameter optimizations are used to maximize the thrust force of both 6-slot/5-pole and 6-slot/7-pole tubular FSPM machines in [5]. The influence of major design parameters can be investigated by individual parameter optimization during optimization. However, whether a global optimization or only a local optimization can be obtained by individual parameter optimization of linear machines depends on the coupling effect of the design parameters, even though the results obtained from the individual parameter optimization and the global optimization of rotary FSPM machines are more or less the same [7]. Therefore, the results from individual parameter optimization of linear machines have to be examined.

Cogging force, which can deteriorate the performance of the linear FSPM machines, has to be minimized as well. A method to reduce cogging force is investigated by fixing assistant teeth on the mover ends is introduced in [8], but only the slot opening associated with assistant teeth is optimized while the width of the assistant tooth is kept the same as the width of stator teeth.

In this paper, a 6-slot/5-pole linear FSPM machine, with particular reference to the planar format, is investigated by FE analyses. The thrust force with a constant copper loss is firstly optimized by individual parameter optimization. A global optimization of thrust force with the same copper loss is obtained by genetic algorithm and used to validate the individual parameter optimization. Furthermore, the parameters of the assistant teeth on the mover ends, including not only the slot opening associated with assistant teeth but also the assistant teeth tips, are optimized to reduce the cogging force.

II. INDIVIDUAL PARAMETER OPTIMIZATION OF THRUST FORCE

The original 6-slot/5-pole linear FSPM machine used for optimization is shown in Fig.1. All the constant values used for optimization are listed in Table I, as shown in Fig.2. In order to simplify the manufacture of the machine, the shape of mover tooth tip is shown in Fig.3. The copper loss of the machine is kept at 30W during the optimization. The total height of the machine h_{th} is kept at 25mm and the length of machine in Z-direction l_z is kept at 80mm. The mover tooth width b_t, the mover back-iron thickness b_{mi} and the stator pole width b_p are assumed to be equal to the mover tooth tip width b_{tt}, as the initial value. The initial value of the stator pole height h_p is assumed to be half of the stator height h_s as the initial value.

The definitions of optimization variables, which include the split ratio between the mover and stator A_s, the stator pole width ratio b_{p_ratio}, the stator pole height ratio h_{p_ratio}, the mover back-iron thickness ratio b_{mi_ratio} and the mover tooth width ratio b_{t_ratio}, are defined as follows:

$$A_s = h_s / h_{th} \tag{1}$$

978-1-4244-8218-4/10/$26.00 ©2010 IEEE

$$b_{p\_ratio}=b_p/\tau_s \quad (2)$$

$$h_{p\_ratio}=h_p/h_s \quad (3)$$

$$b_{mi\_ratio}=b_{mi}/(h_{th}\text{-}g\text{-}h_s) \quad (4)$$

$$b_{t\_ratio}=b_t/b_{mp} \quad (5)$$

The constraints and initial values of the optimization variables are listed in Table I.

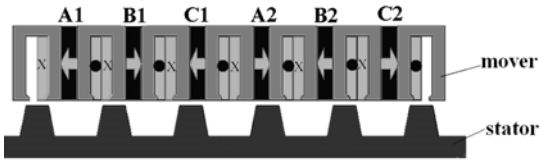

Fig.1 Schematics of 6-slot/5-pole linear FSPM motor.

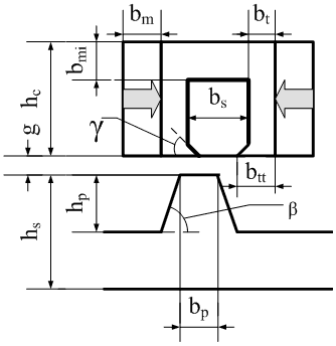

Fig.2 One module of linear FSPM machine for optimization.

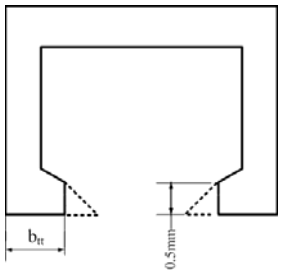

Fig.3 Shape of the mover tooth tip.

TABLE I

Constant values for optimization

Item	symbol	value	Unit
Air-gap length	g	1.0	mm
Magnet thickness	b_m	3.0	mm
Mover tooth tip angle	γ	45	degree
Mover tooth tip width	b_{tt}	3.0	mm
Mover slot pitch	b_{mp}	12	mm
Total height	h_{th}	25	mm
Bottom angle of stator pole	β	arctg4	degree
Stator pole pitch	τ_s	14.4	mm
Machine length(Z-direction)	l_z	80	mm
Magnet remanence	B_r	1.20	T
Magnet relative permeability	μ_r	1.034	
Number of phases		3	
Rated velocity		4.8	m/s
Copper loss		30	W
Winding packing factor	k_p	0.63	
Diameter of the wire	D	1	mm
Resistivity of copper	ρ	1.7×10^{-5}	Ω•mm

TABLE II

Optimization variables and their constrains

Optimization variables	Symbol	Initial value	constraints
Split ratio	$A_s(h_s/h_{th})$	0.5	[0.2,0.7]
Stator pole width ratio	$b_{p\_ratio}(b_p/\tau_s)$	0.21	[0.1,0.4]
Stator pole height ratio	$h_{p\_ratio}(h_p/h_s)$	0.5	[0.3,0.8]
Mover back-iron thickness ratio	b_{mi_ratio} $(b_{mi}/(h_{th}\text{-}g\text{-}h_s))$	0.26	[0.1,0.4]
Mover tooth width ratio	$b_{t\_ratio}(b_t/b_{mp})$	0.25	[0.1,0.3]

The variables in Table II are individually optimized, i.e. only one parameter varies while others are kept constant and the copper loss is always fixed at 30W. The average force in the following optimizations is the average value of the forces in X-direction when the mover moves over a displacement of 360 electrical degrees at a step of 12 electrical degrees toward X-direction from the initial position shown in Fig.1. Each individual optimization follows the optimizing sequence of split ratio, A_s, stator pole width ratio, b_{p_ratio}, stator pole height ratio, h_{p_ratio}, mover back-iron thickness ratio, b_{mi_ratio}, and mover tooth width ratio, b_{t_ratio}, i.e. when one individual parameter is optimized and will be used in subsequent individual parameter optimization.

The split ratio, A_s, is an important parameter in the machine design. Figs. 4-8 show the variation of the average force individually with the split ratio, stator pole width ratio, stator pole height ratio, mover back-iron thickness ratio, and mover tooth width ratio, respectively. As will be seen, the individually optimized A_s is ~0.25, which is much smaller than the tubular FSPM machine [5], the individually optimized b_{p_ratio} is ~ 0.34, which is similar to tubular FSPM machines [5] and rotary FSPM machines [9]. Other individually optimized parameters are $h_{p\_ratio} \approx 0.6$, $b_{mi\_ratio} \approx 0.13$ and $b_{t\_ratio} \approx 0.2$.

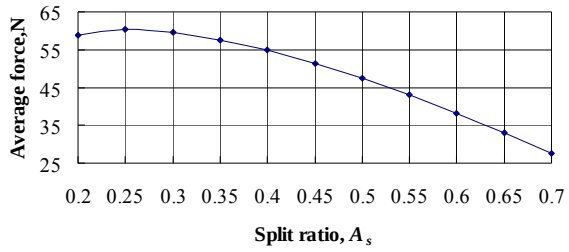

Fig.4 Variation of average force with split ratio.

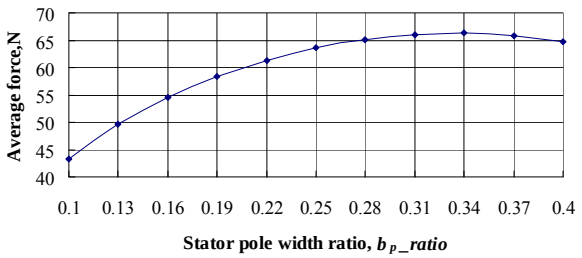

Fig.5 Variation of average force with stator pole width ratio.

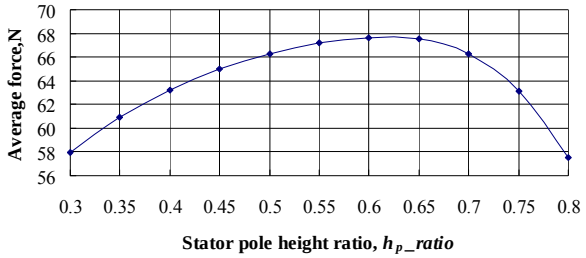

Fig.6 Variation of average force with stator pole height ratio

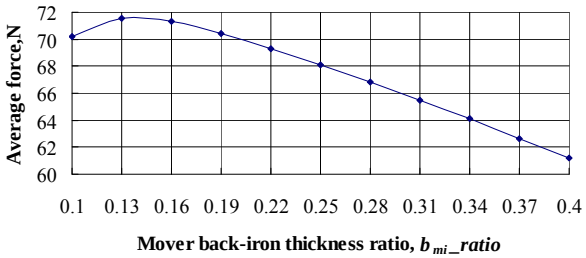

Fig.7 Variation of average force with mover back-iron thickness ratio

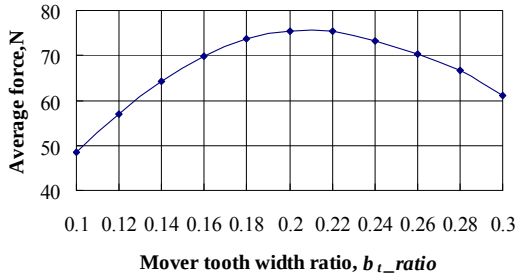

Fig.8 Variation of average force with mover tooth width ratio.

III. GLOBAL OPTIMIZATION OF THRUST FORCE AND COMPARISON

The objective of the global optimization is to minimize the cost function as follows:

$$Cost = - avg\_force \quad (6)$$

The avg_force is the average value of the forces (unit: N) in X-direction when the mover moves over a displacement of 360 electrical degrees at a step of 12 electrical degrees from the initial position shown in Fig.1. The global optimization has been carried out by employing a genetic algorithm and FE model. The population size is 20, and the maximum generation is 23. The other parameters are set as follows. The crossover type is simulated binary crossover. Individual crossover probability, variable crossover probability and Mu all take the value of 1. Variable exchange probability takes 0. Mutation type is polynomial mutation and uniform mutation probability takes 0. Variable mutation probability takes 1. Individual mutation probability takes 1. Standard deviation takes 0.05. Number of survivors from pare to front takes 7.

The genetic algorithm iteration process is revealed in Fig.9. The cost function has a minimum of -76.439 when A_s = 0.2617, b_p_ratio = 0.3042, h_p_ratio = 0.691, b_{mi}_ratio = 0.1412, and b_t_ratio = 0.2052.

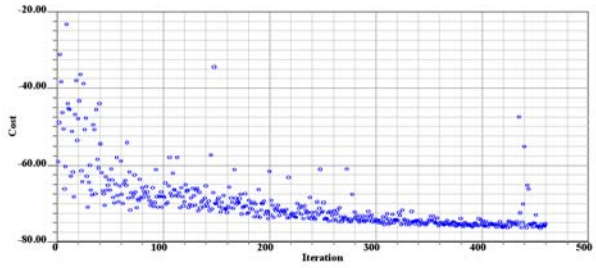

Fig.9 Generation iteration process

The results of individual parameter optimization and global optimization are compared in Table III. Fig. 10 compares the back-EMF waveforms of initial and individually optimized parameters at 4.8m/s. It can be seen that the peak value of back-EMF in individually optimized model is about three times of the initial model.

TABLE III

Initial parameters and optimized parameters

Optimization parameter	Symbol	Initial value	Individually optimized	global optimized
Split ratio	$A_s(h_s/h_{th})$	0.5	0.25	0.2617
Stator pole width ratio	b_p_ratio (b_p/τ_s)	0.21	0.34	0.3042
Stator pole height ratio	h_p_ratio (h_p/h_s)	0.5	0.6	0.691
Mover back-iron thickness ratio	b_{mi}_ratio $(b_{mi}/(h_{th}\text{-}g\text{-}h_s))$	0.26	0.13	0.1412
Mover tooth width ratio	b_t_ratio (b_t/b_{mp})	0.25	0.2	0.2052
Peak back-EMF of phase B, V		9.63	26.17	24.93

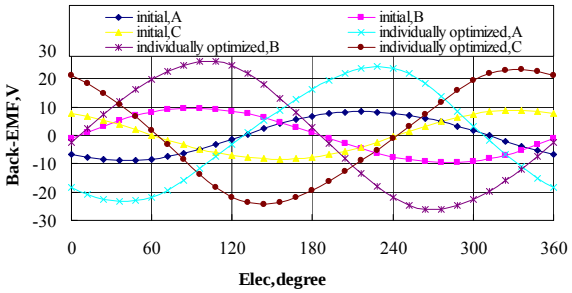

Fig.10 Back-EMF waveforms of initial and individually optimized parameters, 4.8m/s.

Figs.11-13 show the 3-phase (A, B and C) back-EMF waveforms (at a speed of 4.8m/s), cogging forces, and thrust forces for a fixed copper loss of 30W with the individually optimized parameters and the global optimized parameters when the mover moves from the position shown in Fig.1. It can be found that the differences of back-EMF between the individually optimized and global optimized models are very small but the peak to peak value of cogging force with the individually optimized parameters is 20% smaller than that with global optimized parameters.

Fig.14 shows the predicted average force-current density characteristics with the initial, individually optimized and the global optimized parameters, under I_d=0 control. It can be seen that the differences of force characteristics between the

models with individually optimized and the global optimized parameters are very small. Hence, the individual parameter optimization may be employed in optimizing such linear FSPM motor. The output power density of individually optimized machine is 2.236×10^6 W/m^3, which is much larger than that, 1.412×10^6 W/m^3, in the initial machine, when the speed of the mover is at 4.8m/s, the copper loss is kept at 30 W and the stator is assumed to be the same length as the mover for the machine volume calculation.

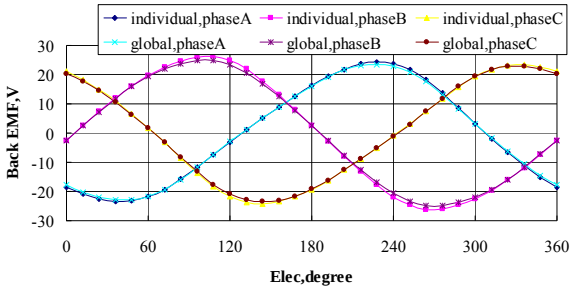

Fig.11 Back-EMF waveforms of individual parameters optimization and global optimization, 4.8m/s.

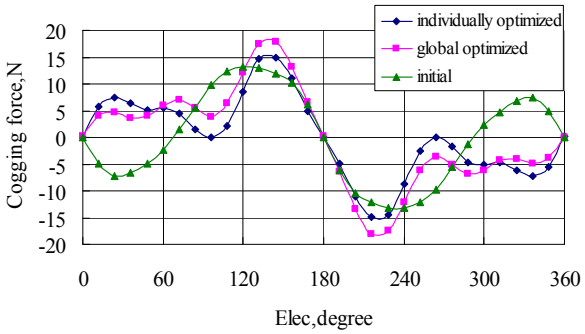

Fig.12 Cogging forces of initial, individual optimized and global optimized parameters.

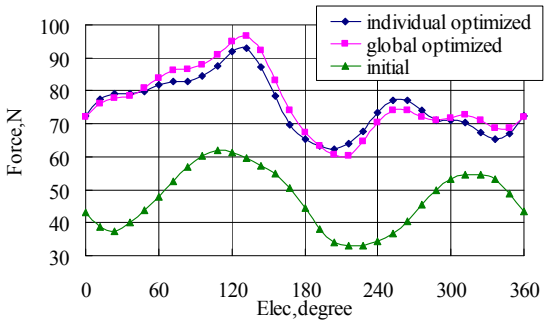

Fig.13 Thrust forces of the three models, 4.8m/s and copper loss=30W

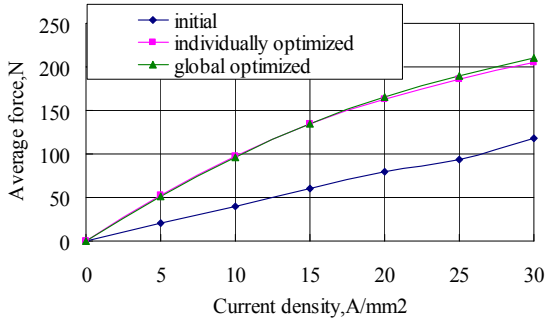

Fig.14 Average force characteristics, winding packing factor=0.63.

IV. Minimization of Cogging Force

It can be seen from Fig.13 that the cogging force in the linear FSPM is large, which contributes significantly to the resultant force ripple. In order to minimize the cogging force of the linear FSPM machine, the slot opening associated with the assistant end teeth (both right and left ends) and the width of assistant tooth tips are optimized by individual parameter optimization. The model with the parameters obtained by individual parameter optimization for larger thrust force, which are list in Table I and Table III, is used as the original model shown in Fig.15, which has a smaller cogging force than the model with global optimized parameters (shown in Fig.13). The definitions of optimization variables, which include the ratio of slot openings associated with the left and right assistant teeth L_{ls}_ratio and L_{rs}_ratio, are as follows:

$$L_{ls}\_ratio = L_{ls}/\tau_s \quad (7)$$

$$L_{rs}\_ratio = L_{rs}/\tau_s \quad (8)$$

Fig.15 Optimization variables for minimum cogging force.

The constraints and initial values of the cogging force optimization variables are listed in Table IV. The left and right end assistant teeth widths are kept at 2.4mm which are obtained from the individual parameter optimization, while the slot opening and the tooth tip are both varying.

TABLE IV

Cogging force optimization variables and their constraints

Optimization variables	Symbol	Initial value	constraints
Ratio of slot opening associated with the left assistant end teeth	L_{ls}_ratio (L_{ls}/τ_s)	0.208	[0.104,1.104]
Ratio of Slot opening associated with the right assistant iron tooth	L_{rs}_ratio (L_{rs}/τ_s)	0.208	[0.104,1.104]
Width of assistant iron tooth tips	L_{tt}	3	[2.4,4.4]

The objectiveness of the cogging force optimization is to minimize the peak to peak value of cogging force. Each individual optimization follows the sequence of optimizing left assistant iron tooth slot opening ratio, L_{ls}_ratio, right assistant iron tooth slot opening ratio L_{rs}_ratio, and assistant iron tooth tips length L_{tt}. Once one individual parameter is optimized, it will be used in subsequent individual parameter optimization.

Figs. 16-18 show the variation of peak to peak value of cogging force individually with the left assistant iron tooth slot opening ratio, right assistant iron tooth slot opening ratio, and assistant iron tooth tips length, respectively. The peak to peak value of cogging force with the assistant iron teeth slot opening varies periodically with the stator pitch, so only one period is given in Fig.16 and Fig.17.

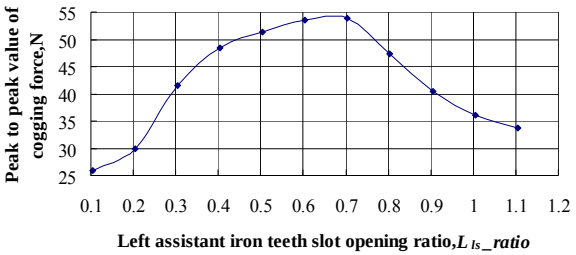

Fig.16 Variation of peak to peak cogging force with L_{ls}_ratio

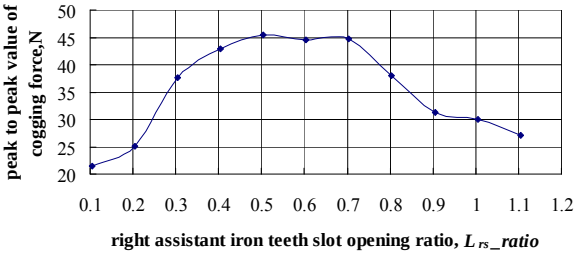

Fig.17 Variation of peak to peak cogging force with L_{rs}_ratio.

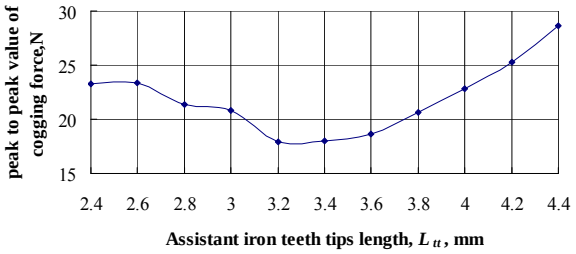

Fig.18 Variation of peak to peak cogging force with L_{tt}

All the parameters obtained by optimization are listed in Table V. Fig.19 shows the FE predicted open-circuit field distributions of the model with the optimized parameters. Figs. 20-22 show the cogging force, back-EMF and force with initial and optimized parameters when the mover moves from the position shown in Fig.15. It can be seen that the peak to peak value of the cogging force of the model with optimized parameters is about 40% smaller than the initial model while the back EMF is nearly the same.

TABLE V

Initial parameters and optimized parameters of cogging force optimization

Optimization variables	Symbol	Initial value	Optimized value
Left assistant teeth slot opening ratio	L_{ls}_ratio (L_{ls}/τ_s)	0.208	0.104
Right assistant teeth slot opening ratio	L_{rs}_ratio (L_{rs}/τ_s)	0.208	0.104
Width of assistant teeth tips	L_{tt}	3	3.2

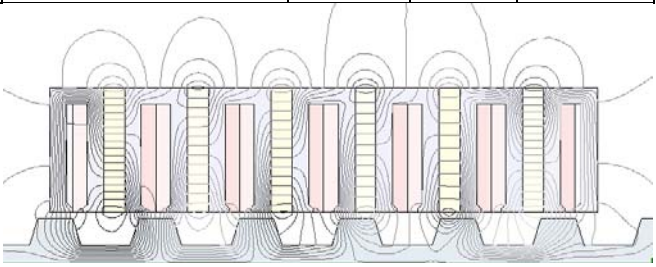

Fig.19 Open-circuit field distributions

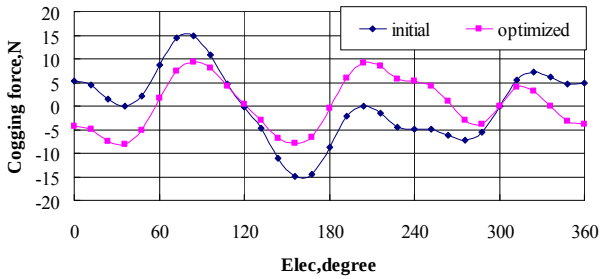

Fig.20 Cogging force of models with initial and optimized parameters.

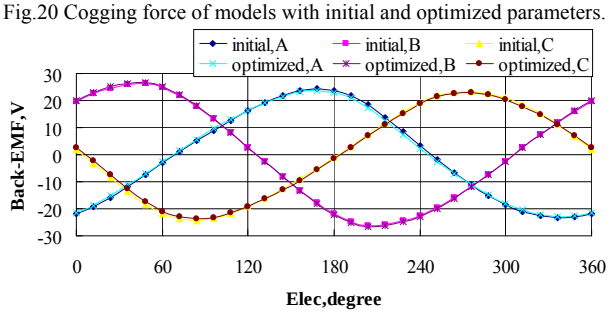

Fig.21 Back-EMF of model with initial and optimized parameters,4.8m/s

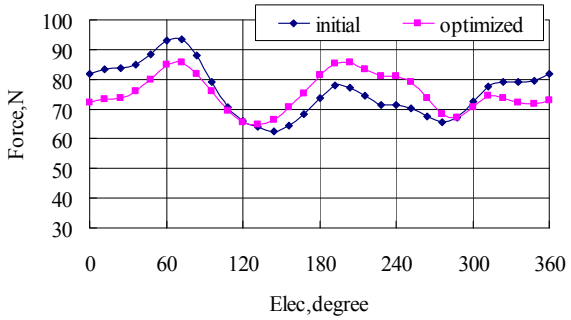

Fig.22 Thrust forces of the two models, 4.8m/s and copper loss=30W

V. CONCLUSIONS

A 6-slot/5-pole linear FSPM machine, with particular reference to the planar format, is studied in this paper. The influence of major design parameters, such as the split ratio, the stator pole width, the stator pole height, the mover back-thickness and the mover tooth width, on the thrust force, is investigated by the FE analyses when the copper loss is fixed. A global optimization of thrust force is obtained by genetic algorithm, and compared with the optimization obtained by individual parameter optimization. The difference between the two optimizations is very small, and hence global optimization may be obtained by individual parameter optimization of linear FSPM machine. The slot opening associated with the assistant end tooth and the width of assistant tooth tips are optimized and the peak to peak value of the cogging force is reduced by about 40% without influencing the back EMF.

The analysis should be applicable to linear FSPM machines having other mover slot/stator pole combinations or winding connections.

VI. ACKNOWLEDGEMENT

The first author, W. Min, gratefully acknowledges the

China Scholarship Council for providing financial support for a one-year visiting PhD studentship at The University of Sheffield.

REFERENCES

[1] T. Kenjo, and A. Sugawara, "Stepping motors and their microprocessor controls," Clarendon Press, Oxford, 1994.

[2] W. E. Hinds, and B. Nocito, "The Saywer linear motor," *Proc. 3th Annu. Symposium on Incremental Motion Control Systems and Devices*, University of Illinois, 1974, pp. W1-10.

[3] R. C. Okonkwo, "Design and performance of permanent-magnet DC linear motors," *IEEE Trans. Magn*., vol. 42, no. 9, 2006.

[4] C. F. Wang, J. X. Shen, L. L. Wang, and K. Wang, "A novel permanent magnet flux-switching linear motor," *Proc. 4th IET Conf. on Power Electronics, Machines and Drives (PEMD'2008)*, pp. 116-119, 2008.

[5] Z. Q. Zhu, X. Chen, J. Chen, D. Howe, and J. Dai, "Novel linear flux switching permanent magnet machines," *in Int. Conf. Electrical Machines and Systems*, Oct. 17–20, 2008, pp. 2948–2953.

[6] J. B. Wang, W. Y. Wang, K. Atallah, and D. Howe, "Design considerations for tubular flux-switching PM machines," *IEEE Trans.Magnetics*, vol.44, no.11, pp.4026-4032, 2008.

[7] Z. Q. Zhu, Y. Pang D. Howe, S. Iwasaki, R. Deodhar, and A. Pride,"Analysis of electromagnetic performance of flux-switching permanent magnet machines by nonlinear adaptive lumped parameter magnetic circuit model," *IEEE Trans.Magnetics*, vol.41,no.11, pp.4277-4287, 2005.

[8] C. F. Wang, J. X. Shen, Y. Wang, L. L. Wang, and M. J. Jin, "A new method for reduction of detent force in PM flux-switching linear motors," *IEEE Trans. Magnetics*, vol.45, no.6, pp.2843-2846, 2009.

[9] J. T. Chen, Z. Q. Zhu, A. S. Thomas, and D. Howe, "Optimal combination of stator and rotor pole numbers in flux-switching PM brushless AC machines," *Proc. Int. Conf. on Electrical Machines and Systems (ICEMS'2008)*, Oct. 2008, Wuhan, China.